

Influence of interface structure on electronic properties and Schottky barriers in Fe/GaAs magnetic junctions

D. O. Demchenko and Amy Y. Liu

Department of Physics, Georgetown University, Washington, DC 20057-0995, U.S.A.

(Dated: October 9, 2018)

The electronic and magnetic properties of Fe/GaAs(001) magnetic junctions are investigated using first-principles density-functional calculations. Abrupt and intermixed interfaces are considered, and the dependence of charge transfer, magnetization profiles, Schottky barrier heights, and spin polarization of densities of states on interface structure is studied. With As-termination, an abrupt interface with Fe is favored, while Ga-terminated GaAs favors the formation of an intermixed layer with Fe. The Schottky barrier heights are particularly sensitive to the abruptness of the interface. A significant density of states in the semiconducting gap arises from metal interface states. These spin-dependent interface states lead to a significant minority spin polarization of the density of states at the Fermi level that persists well into the semiconductor, providing a channel for the tunneling of minority spins through the Schottky barrier. These interface-induced gap states and their dependence on atomic structure at the interface are discussed in connection with potential spin-injection applications.

PACS numbers: 73.20.At, 75.70.Cn, 73.30.+y, 72.25.Mk

I. INTRODUCTION

The problem of spin injection has been a subject of intense study since the proposal of the electronic analog of the electro-optic modulator.¹ Since then the entire field of spintronics has been developed. The main idea lies in the possibility of controlling the spin of charge carriers, thereby adding an additional degree of freedom to existing semiconductor-based electronics. A number of novel electronics devices based on this idea have been proposed, such as reprogrammable logic devices, spin valves, spin-injection diodes, and devices utilizing giant magnetoresistance (see, for instance, Ref. 2). A major challenge in the field has been the creation of spin-polarized currents in nonmagnetic semiconductors. One approach is the use of ferromagnetic contacts as spin sources. A spin polarization of the current is expected from the different conductivities resulting from the different densities of states for spin-up and spin-down electrons in the ferromagnet. Significant progress in molecular beam epitaxy has allowed growth of high quality, virtually defect-free junctions between magnetic materials and semiconductor substrates, and films of ferromagnetic metals such as Fe or Co grown epitaxially on semiconductor structures are promising candidates for spin injection.

Zhu and co-authors³ have demonstrated efficiencies of 2% for injection of spin-polarized electrons from a metal into a semiconductor for a GaAs/(In,Ga)As light emitting diode (LED) covered with Fe. Moreover, Hanbicki *et al.*⁴ have managed to achieve a spin injection efficiency of 30%. In the latter case, an Fe film grown on an AlGaAs/GaAs quantum well LED structure was used. In both cases it was suggested that the spin injection arises from tunneling of spin-polarized electrons from the metal into the semiconductor across the Schottky barrier formed at the interface. Such a tunneling process is believed to be responsible for the spin injection since it is

not affected by the conductivity mismatch⁵ between the metal and semiconductor that severely limits the spin-injection efficiency in the diffusive transport regime. A remarkable consequence of such a mechanism is that it is independent of temperature. In fact, in Refs. 3 and 4, nearly constant tunneling efficiencies of 2% and 30% were observed for a range of temperatures from 2 K to 300 K and from 90 K to 240 K, respectively. Recently spin injection efficiencies of 13% have been reported at 5 K across a Fe/GaAs(110) interface,⁶ and 6% across a Fe/Al_xGa_{1-x}As/GaAs Schottky contact at 295 K.⁷ At the moment, the room temperature record of 32% is held by CoFe/MgO injectors grown on *p*-GaAs(100) substrates.⁸

The electronic structure of the metal/semiconductor interface plays an important role in spin-dependent transport properties across such junctions. For the case of the Fe/GaAs(001) interface, a number of first-principles studies have been carried out. Green's function methods have been used to study the electronic structure, charge transfer, and spin polarization in Fe/GaAs/Fe(001) tunnel junctions in which the interface geometry is atomically abrupt and ideal.^{9,10,11} It was noted that the calculated magnetic properties at the interface are sensitive to the interface structure, indicating that structural relaxations could be important.¹⁰ Other studies have focused on the initial stages of growth of Fe on GaAs and have considered how structural relaxation and intermixing of metal and semiconductor atoms affect magnetic properties of thin films of Fe on GaAs.^{12,13,14} Still lacking is an understanding of how details of the atomic arrangement at the interface affect properties directly relevant to spin injection, such as Schottky barrier heights and the nature of the interface-induced states in the semiconductor gap through which spins may tunnel. In this paper, we address this by considering structural models for the (001) interface between Fe and GaAs that allow for dif-

ferent degrees of intermixing and relaxation. The effects of interface structure on potential, charge, and magnetization profiles, Schottky barrier heights, spin-polarized densities of states, and interface-induced gap states are investigated. The results are discussed in connection with potential spin-injection applications.

The paper is organized in the following way. Computational details are given in Section II. In Section III we describe and discuss the structures considered and the resulting structural, electronic, and magnetic properties. Conclusions are presented in Section IV.

II. COMPUTATIONAL DETAILS

The bulk lattice constants of bcc Fe (2.866 Å) and zincblende GaAs (5.654 Å) differ by almost exactly a factor of two. Therefore, an interface consisting of a (001) Fe slab placed on the (001) surface of GaAs has a lattice mismatch of 1.36%. The close lattice match helps keep the concentration of defects at such interfaces relatively low. In this work, interfaces were modeled using supercells consisting of nine layers of Fe and nine layers of semiconductor atoms (five As and four Ga, or vice versa, depending on the semiconductor surface termination.) This is sufficient to ensure that the adjacent interfaces do not interact with each other, as confirmed by both total energy calculations and macroscopic averages of the electrostatic potential and charge.

The calculations were performed with the VASP program,¹⁵ an *ab initio* density functional code that uses the planewave pseudopotential method. The generalized gradient approximation was used to treat the exchange-correlation part of the electron-electron interaction.^{16,17} All calculations employed ultrasoft pseudopotentials¹⁸ and planewave basis sets with a kinetic energy cut off of 370 eV. Monkhorst-Pack meshes¹⁹ of $8 \times 8 \times 4$ \mathbf{k} -points were used to sample the Brillouin zone, and Gaussian smearing of electronic states ($\sigma = 0.2$ eV) was used to achieve faster convergence of Brillouin zone sums with respect to the number of \mathbf{k} -points.

III. RESULTS

A. Structure

The Fe/GaAs interface structures considered in this work are shown in Fig. 1. While the bare GaAs(001) surface reconstructs to form dimers on the surface,²⁰ recent calculations suggest that these dimers become unstable upon adsorption of Fe.¹² Therefore, in this work, we consider 1×1 interfaces only. We assume the Fe(001) and GaAs(001) slabs are aligned so that in the first complete metal layer, sites that would have been occupied by semiconductor atoms in the absence of the interface are now occupied by metal atoms. An abrupt interface like this with no intermixing of metal and semiconductor atoms

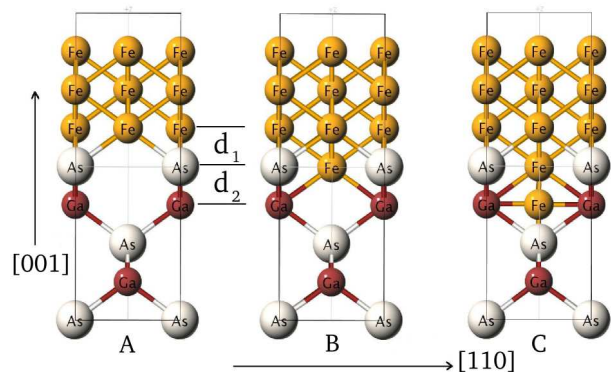


FIG. 1: Three models for the structure of the 1×1 interface between As-terminated GaAs(001) and Fe(001) surfaces. Model A is an abrupt interface, model B has one layer containing both metal and semiconductor atoms, and model C has two intermixed layers.

will be referred to as model A (as in Ref. 12). In model B, the bcc metal structure is partially continued into the first semiconductor layer so that metal atoms occupy sites that are normally empty in the first layer of the semiconductor. In model C, metal atoms occupy interstitial sites in the second semiconductor layer as well. Both As- and Ga-terminated interfaces can be grown experimentally, and therefore, both are considered here. We find that for the supercells of the size considered in this work, model C is never energetically favorable. This agrees with Ref. 12, where it was found that model C has lower energy only for coverages of Fe not exceeding two monolayers. Therefore we focus on models A and B.

The comparison of total energies of models A and B is not physically meaningful since the interfaces have different numbers of atoms. The formation energies of these models are, on the other hand, physically comparable and given by

$$E_{form} = E_t - \sum_i N_i \mu_i. \quad (1)$$

Here, E_t is the total energy of the supercell, N_i is the number of atoms of the type i in the cell, and μ_i is the chemical potential of the i -th atom. Thus, all energies from the model B calculations were adjusted by twice the value of the chemical potential for Fe, since each supercell contains two equivalent interfaces. Test calculations of the formation energy using supercells with one A interface and one B interface confirm that the supercells are large enough to ensure that the interaction between interfaces is negligible.

Since electronic and magnetic properties may differ significantly as a result of small changes in structural parameters, we have relaxed all the interface models considered. In our calculations the interfaces were relaxed with respect to two parameters: the distance between the adjacent Fe and As (or Ga) layers, d_1 , and the distance between the first two layers in the GaAs slab, d_2 (see Fig.

TABLE I: Interlayer relaxations, in units of the GaAs lattice constant a_0 . Here, Δd_1 is the difference between the relaxed and ideal ($0.25a_0$) separation of adjacent Fe and As (Ga) planes at the interface, and Δd_2 is the change in the distance between the first two planes in the GaAs slab.

	As-terminated		Ga-terminated	
	Δd_1	Δd_2	Δd_1	Δd_2
Model A	0.0	0.025	0.022	0.017
Model B	0.017	0.068	0.018	0.058

1). The in-plane lattice constant was fixed at the bulk GaAs value, $a_0 = 5.654 \text{ \AA}$. The results of the relaxation are presented in Table I. For As-terminated model A, the distance between As and Fe planes remains at the ideal value of $0.25a_0$, while the separation between the first plane of As and the adjacent plane of Ga is stretched by 10%. With Ga-termination, both d_1 and d_2 increase by similar amounts in model A. In model B, which has the intermixed layer, the first two planes of the semiconductor slab are repelled considerably farther apart, regardless of the termination. It was previously pointed out that lowering the concentration of atoms in the interface region is energetically favorable in model B, since the electrons from the extra Fe atoms in the intermixed layer fill antibonding orbitals and weaken the interface bonding.¹²

The results of the formation energy calculations for the ideal and relaxed interfaces are summarized in Table II. For both ideal and relaxed geometries, model A is energetically favored for As-terminated interfaces, and model B is favored for Ga-terminated interfaces. This results from an interplay between optimization of the coordination of the metal and semiconductor atoms and the relative strengths of the metal-cation and metal-anion bonds. Because of stronger pd hybridization, the Fe-As bond is more stable than the Fe-Ga bond.¹³ For model A, the interface Fe site is six-fold coordinated, with four Fe neighbors in the second metal layer and two semiconductor neighbors in the first semiconductor layer. While putting Fe atoms in interstitial sites in the first semi-

TABLE II: Formation energy differences, in eV per 1×1 interface unit cell. With As-termination, the abrupt interface of model A is favored, while with Ga-termination, the intermixed interface of model B is preferred.

	As-terminated	Ga-terminated
	Ideal - Relaxed	Ideal - Relaxed
Model A	0.046	0.059
Model B	0.282	0.291
	Model A - Model B	Model A - Model B
Ideal	-0.400	0.318
Relaxed	-0.164	0.551

conductor layer fully coordinates the interface Fe sites in model B, it also significantly weakens the bonding between the first two semiconductor layers, which become overcoordinated. At the As-terminated interface, the strong Fe-As bonds compensate for the undercoordination of the Fe sites, making model A favorable, while at the Ga-terminated interface, the weak interaction between Fe and Ga favors full coordination of Fe interface sites, as in model B.

B. Schottky Barriers and Electronic Structure

Figure 2 shows the calculated site-projected densities of states (DOS) for atoms in different layers in the relaxed As-terminated model A. The general features are similar for all the structural models considered. The DOS in the most bulk-like layers of the supercell closely resembles the DOS of bulk Fe or GaAs. Near the interface, a peak develops in the DOS at the Fermi level. The peak is largest in the first Fe layer and decreases into both the GaAs and Fe slabs. In the first few GaAs layers, states spread throughout the entire band gap of bulk GaAs, though the gap is practically recovered in the layer farthest from the interface. Bardeen²¹ estimated that surface states with density $\sim 10^{13} \text{ eV}^{-1} \text{ cm}^{-2}$ would effectively pin the Fermi level close to the charge neutrality level in the semiconductor gap. Our calculations for the relaxed As-terminated model A, for example, yield values of DOS at the Fermi level of $\sim 2 \times 10^{15} \text{ eV}^{-1} \text{ cm}^{-2}$ in the first Fe layer, and $\sim 1 \times 10^{14} \text{ eV}^{-1} \text{ cm}^{-2}$ in the first two layers of the GaAs slab. These may be sufficient to pin the Fermi level, which consequently affects the Schottky barrier height (SBH). We will return to examine the nature of these mid-gap states, their spin polarization, and their role in spin tunneling in section D.

As mentioned, Schottky barriers may be a necessary mechanism for overcoming the conductivity mismatch for the injection of spin from a ferromagnetic metal into a semiconductor. Schottky barrier heights can be evaluated from first principles using a macroscopic average method combined with the supercell approach.²² Two necessary conditions are: 1) the supercell contains two equivalent interfaces, which eliminates any electric fields that might be present due to unbalanced charges, and 2) the supercell is sufficiently large so the bulk charge and potential properties are recovered in the most bulk-like layers of the supercell. In such a way an isolated interface is accurately modeled using a supercell.

The calculation of the p -type Schottky barrier height, ϕ_p , is split into two parts:

$$\phi_p = \Delta E_v + \Delta V. \quad (2)$$

The band structure term,

$$\Delta E_v = E_F - E_v, \quad (3)$$

is the difference between the Fermi level E_F in the metal and the valence band edge in the semiconductor E_v ,

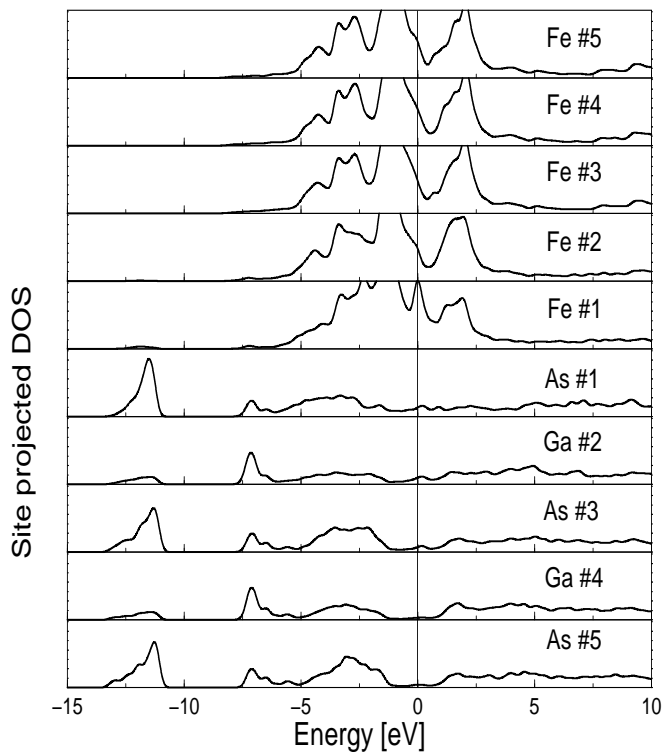


FIG. 2: Site-projected densities of states for atoms in different atomic layers of the relaxed GaAs/Fe(001) supercell with As-terminated model A interfaces. The bottom panel represents the semiconductor layer farthest from the interface (As #5), and the top panel represents the most bulk-like layer of Fe (Fe #5). The vertical line at zero energy indicates the Fermi level. In each panel, the vertical scale runs from 0 to 1.8 states/eV/atom.

where each is measured with respect to the average electrostatic potential in the corresponding bulk material. The band structure term is calculated from separate bulk calculations for the two constituents of the Schottky contact. This term implicitly includes all quantum mechanical effects as well as the exchange-correlation part of the potential.

The other contribution to ϕ_p is the potential line-up across the interface ΔV . This potential line-up is related to the dipole moment of the charge profile,²² depends on the structure of the interface, and therefore cannot be calculated simply from two bulk calculations. It is the difference between the macroscopic averages of the electrostatic potential in two bulk-like regions of the supercell. As an example, Fig. 3 shows the planar average over the $x-y$ plane and the macroscopic average of the electrostatic potential computed for the superlattice with As-terminated relaxed model A interfaces. The macroscopic average lacks the bulk-like oscillations present in the planar average, and thereby allows one to extract the desired potential line-up ΔV . The macroscopic average, however, does not provide reliable information about potential behavior in the close vicinity of the interface since

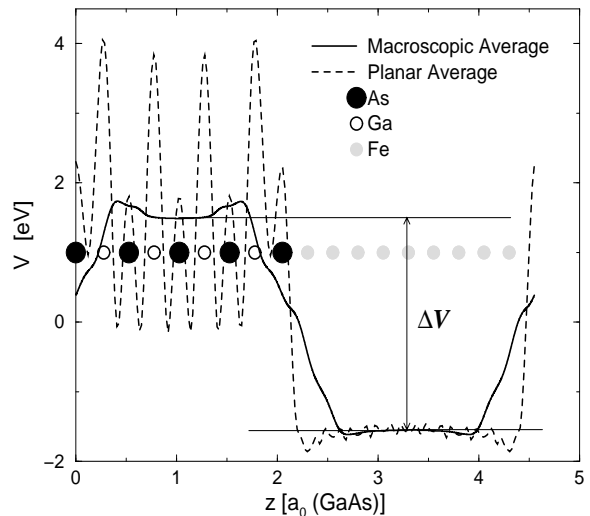


FIG. 3: Planar and macroscopic averages of the electrostatic potential calculated for the relaxed As-terminated model A supercell. The potential is plotted as a function of z , the position of atomic layers along the axis of the supercell. The potential line-up ΔV needed for the Schottky barrier height calculation is given by the difference between the two plateaus in the macroscopically averaged potential.

the resolution of the method is limited to the lattice period, the GaAs lattice constant a_0 in our case. There is a notable difference between the planar average and the macroscopic average in the vicinity of the interface.

We have calculated the p -type SBH for the ideal and relaxed structures described in the previous section. Since it is electrons that are injected from Fe into GaAs in spin injection experiments, the n -type SBH is of more interest. To obtain the n -type SBH from our calculations, we subtract the calculated p -type SBH from the experimental GaAs band gap of 1.52 eV.²³ The results are presented in Table III. The calculated SBH is sensitive to structural changes, and the differences between the SBH values in Table III show the magnitude of changes one can expect for different interface structures. Intermixing of metal and semiconductor atoms at the interface decreases the n -type Schottky barrier height significantly (by about 0.2-0.3 eV), while the effect of inter-layer relaxation is generally weaker. This level of sensitivity of SBH values to interface structure is consis-

TABLE III: Calculated n -type Schottky barrier heights (in eV) for ideal and relaxed geometries. Interfaces with intermixing (model B) have lower barrier heights than abrupt interfaces (model A).

	As-terminated		Ga-terminated	
	Ideal	Relaxed	Ideal	Relaxed
Model A	0.87	0.82	1.01	1.08
Model B	0.58	0.64	0.69	0.89

tent with the observed dependence of measured SBHs on growth conditions. For Fe/GaAs interfaces fabricated by metal evaporation in ultrahigh vacuum, SBHs in the range of 0.72-0.75 eV have been reported.²⁴ More recent experiments on As-terminated atomically clean (001) interfaces grown by molecular beam epitaxy have yielded barriers around 0.90-0.92 eV.^{25,26} In the latter work, the samples had sufficiently low interface defect concentrations that Fermi-level pinning by antisite defects was suppressed.^{25,26} Our calculated results for the energetically favored geometries, i.e. As-terminated relaxed model A and Ga-terminated relaxed model B, are close to the SBH values obtained for these clean samples. Overall, the present results compare more favorably to experiments than earlier density-functional calculations of the p -type SBH at ideal Fe/GaAs (110) interfaces.²⁷

C. Charge Distribution and Magnetic Moments

To investigate the redistribution of charge that gives rise to the Schottky barrier, we have computed the charge within Wigner-Seitz spheres centered on atomic sites.²⁸ We have also compared the planar-averaged charge in the interface region to the planar-averaged charge in the bulk-like regions and to the planar-averaged superposition of atomic charges. The qualitative features of the charge redistribution deduced from the sphere charges are consistent with those suggested by the planar-averaged charge. Figure 4 shows the difference between the charge inside the spheres in the supercell and in the bulk. At the abrupt interface (model A), there is an evident transfer of charge from the interface Fe layer into the semiconducting slab, regardless of the semiconductor termination. In Ref. 10, it was found that for unrelaxed abrupt interfaces, the interface Fe loses more charge to Ga neighbors than to As neighbors. We find that this difference is enhanced when the interlayer distances are allowed to relax. Interface Fe atoms also lose significant charge to the interstitial region where bond formation takes place. The redistribution of charge is limited to regions close to the interface. By the third semiconductor layer, the charge within the spheres has nearly recovered to bulk values.

In model B, Fe sites in the first full Fe layer are fully coordinated, so the local charge around these sites is much closer to the bulk value than in model A. The charge redistribution takes place primarily within the intermixed layer, where the Fe sites are undercoordinated and the semiconductor sites are overcoordinated. While the amount of local charge lost by Fe sites in the intermixed layer is about the same for both terminations ($\sim 0.2e$), with Ga-termination, the Ga sites in the intermixed layer gain electrons while with As-termination, the As interface sites lose electrons, indicating a transfer of charge into interstitial regions in the Fe-As intermixed layer.

Fig. 5 shows the local magnetic moments across the

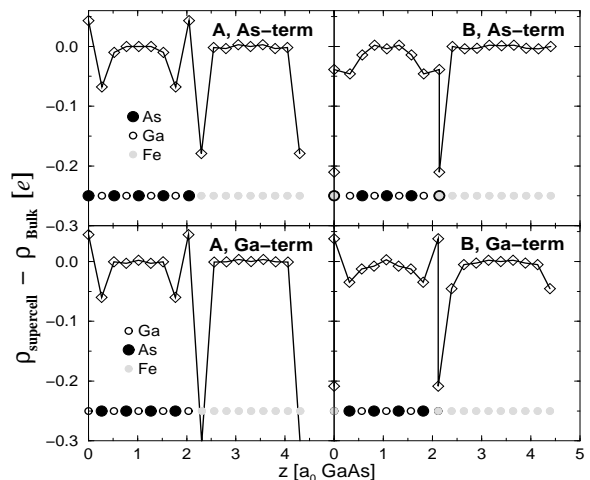


FIG. 4: Difference between the charge inside the atomic spheres for the supercell and bulk GaAs and Fe, plotted as a function of distance z along the direction normal to the interface. The upper panels show results for relaxed As-terminated models A and B, and the lower panels show results for relaxed Ga-terminated models A and B. In the intermixed layer in model B, the higher point represents the charge difference for the As or Ga atom and the lower point represents that for the Fe atom.

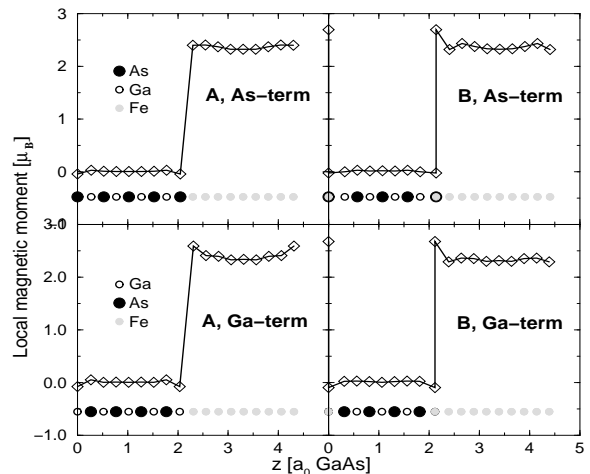


FIG. 5: Local magnetic moments plotted as a function of distance z along the direction normal to the interface. The upper panels show results for relaxed As-terminated models A and B, and the lower panels show results for relaxed Ga-terminated models A and B. In the intermixed layer in model B, the higher data point represents the Fe moment while the lower data point represents the Ga or As moment.

Fe/GaAs interface for all four structurally relaxed models. The magnetic moments were calculated from the integrated spin-polarized DOS within the Wigner-Seitz spheres. There is a small enhancement of the magnetic moment near the Fe interface in comparison to the bulk-like moment of $\sim 2.3\mu_B$ in the central Fe layer. This is similar what was found in Ref.[11]. Since the Fe mo-

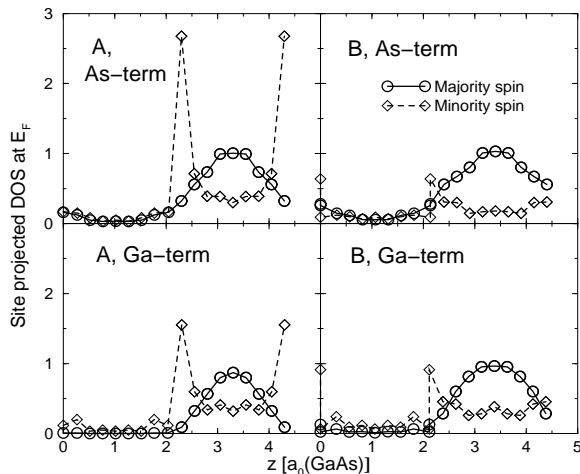


FIG. 6: Local majority-spin (circles) and minority-spin (diamonds) densities of states at the Fermi level in different atomic layers. The top panels show results for relaxed As-terminated models A and B, and the bottom panels show results for relaxed Ga-terminated models A and B. The vertical scale, in units of states/eV/atom, is kept the same in all panels to facilitate comparisons.

ment at the interface is sensitive to the Fe-As(Ga) bond length and can be quenched by reducing the bond length by a few percent,¹³ the relaxation of the interlayer distances near the interface is important. In model A the enhancement of the Fe moment at the interface ranges from $0.1\mu_B$ for As termination to $0.3\mu_B$ for Ga termination. Model B has a larger enhancement of the magnetic moment at the Fe sites located in the intermixed layer, with spin moments $\sim 0.4\mu_B$ larger than at the bulk-like sites. These results, which indicate that Fe is ferromagnetic at the GaAs interface, are consistent with recent experiments on the Fe/GaAs (100)- 4×6 interface²⁹ where bulk-like spin magnetic moments were observed using x-ray magnetic circular dichroism. In our calculations, all four structural models also have small induced opposite magnetic moments in the first semiconductor layer with the approximate values of $0.04\mu_B$ and $0.02\mu_B$ for As-terminated models A and B, respectively, and $0.08\mu_B$ and $0.09\mu_B$ for Ga-terminated models A and B, respectively.

D. Spin-Polarization and Interface States

Figure 6 shows the local majority (spin-up) and minority (spin-down) densities of states calculated at the Fermi energy for the relaxed As- and Ga-terminated models A and B. Each point on the curves corresponds to an atomic layer. In all four cases the majority-spin DOS is largest at the center of the Fe slab and decays monotonically towards and across the interface into the GaAs slab. At the same time the minority-spin DOS exhibits a sharp peak in the vicinity of the interface on the Fe side and

decreases into the center of the Fe slab. In the GaAs slab both majority and minority DOS decay exponentially, but the dominance of the minority states is preserved throughout the GaAs slab. Hence, close to the interface on the Fe side, the spin polarization reverses sign and peaks because of the large difference between spin-up and spin-down density of states. While model B exhibits such a reversal with relatively modest differences between spin-up and spin-down DOS, model A shows significantly larger values of spin polarization.

Similar behavior of the spin-dependent DOS at the Fermi level has been observed both theoretically and experimentally for the free Fe surface.^{30,31} A peak in the scanning tunneling spectra of the Fe(001) surface was attributed to a minority-spin surface band located about 0.3 eV above the Fermi level at the Γ point in the two-dimensional Brillouin zone. We find analogous behavior at the Fe/GaAs interface, with the increase in minority spin DOS at the Fermi level at the interface attributable to d states localized on Fe interface sites. The valence charge density for one of these interface states at the As-terminated abrupt interface is shown in Fig. 7. This $d_{3z^2-r^2}$ -derived Shockley-like state, located about 0.4 eV above the Fermi level at the Γ point, produces high densities of states within the GaAs band gap and decays evanescently into the GaAs slab. At the intermixed interfaces of model B, analogous states localized on the Fe sites in the intermixed layer are found near the Fermi level, but because of the stronger influence of the reduced symmetry of GaAs compared to Fe, some of these interface states are more clearly a mixture of $d_{3z^2-r^2}$ and d_{xy} character, with lobes pointing along the z and $x = \pm y$ directions. (The x and y directions are along the cubic axes of both the bcc Fe and zinc-blende GaAs lattices.)

These interface states likely play a role in Fermi-level pinning, which experimentally manifests as an insensitivity of the SBH to the metal workfunction. Our calculations suggest that at the defect-free interface, the Fermi level is pinned by Fe minority-spin interface states, supporting the metal-induced gap states (MIGS) model^{32,33} rather than the semiconductor surface state model.²¹ This also agrees with recent experiments on the pressure dependence of metal/GaAs Schottky barrier heights,²⁶ which support the MIGS model for atomically clean Fe/GaAs interfaces. A notable difference between the interface states we find and MIGS suggested in the original works^{32,33} is that the interface states in our case are localized at the interface and are not derived from the metal bulk states.

To quantify the decay of the spin polarized DOS into the GaAs, we have performed additional large supercell calculations using the relaxed interface geometries, increasing the number of atomic layers in the GaAs slab to 17. A large number of \mathbf{k} -points was used in the DOS calculations ($24\times 24\times 4$), and a Gaussian broadening of states with $\sigma = 0.1$ eV was used. We fit the DOS at the Fermi level in the GaAs slab to the functional form $e^{-2\kappa z}$, where κ is a decay constant, and z is the distance

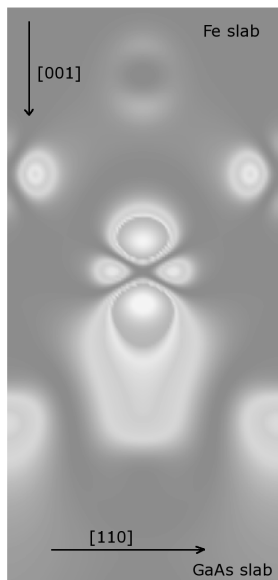


FIG. 7: Valence charge density of a minority-spin interface state at the Γ -point in the relaxed As-terminated model A supercell. The top half of the figure contains Fe layers and the bottom half contains GaAs layers. This state lies about 0.4 eV above the Fermi level.

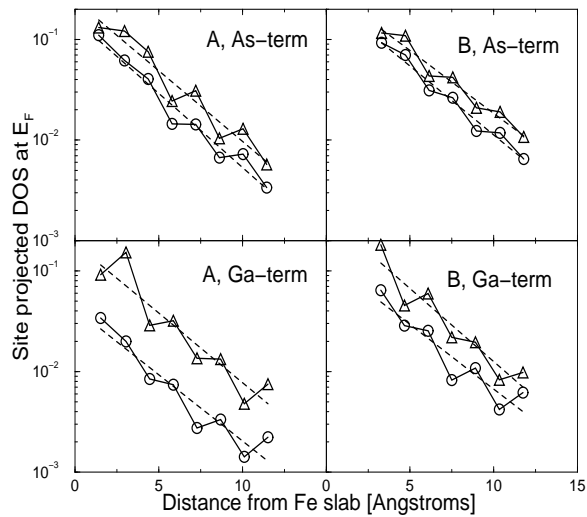


FIG. 8: The site-projected GaAs DOS at the Fermi level as a function of the distance from the Fe slab. The majority-spin DOS are plotted with circles and the minority-spin DOS are plotted with triangles. The upper panels correspond to As-terminated models A and B, and the lower panels correspond to Ga-terminated models A and B. The DOS are in units of states/eV/atom.

from the interface. The decay constants $\kappa_{\uparrow,\downarrow}$ for states with different spin, and corresponding decay lengths $l_{\uparrow,\downarrow}$, are listed in Table IV. Semi-logarithmic plots of the majority- and minority-spin DOS at the Fermi level in the GaAs slab are shown in Fig. 8, along with the fitted exponentials (dashed lines). Each point corresponds

to an atomic layer, and data corresponding to the intermixed layer in model B was omitted since this layer contains both Fe and semiconductor atoms. At the Fermi level the minority-spin states continue to dominate the majority-spin states throughout the GaAs slab. There is a significant proximity effect in the sense that the *ratio* of the DOS corresponding to the two spin states does not change significantly. In other words, the spin polarization of the states at the Fermi level remains virtually constant into the bulk of GaAs, even as the magnitude of the DOS decays exponentially.

TABLE IV: Decay constants $\kappa_{\uparrow,\downarrow}$ (in \AA^{-1}) for majority and minority states and corresponding decay lengths $l_{\uparrow,\downarrow}$ (in \AA).

	As-terminated		Ga-terminated	
	κ_{\uparrow}	κ_{\downarrow}	κ_{\uparrow}	κ_{\downarrow}
Model A	0.17	0.16	0.15	0.16
Model B	0.16	0.14	0.15	0.18
	l_{\uparrow}	l_{\downarrow}	l_{\uparrow}	l_{\downarrow}
Model A	3.0	3.1	3.3	3.1
Model B	3.2	3.5	3.4	3.0

The calculated decay constants $\kappa_{\uparrow,\downarrow}$ listed in Table IV show that there is not a significant difference between the decay of spin-up and spin-down states for a given structure geometry. Such behavior is expected (assuming that the effective masses of spin-up and spin-down electrons do not differ significantly) since states of the same energy should have the same decay constants unless the potential barriers for the two particles differ. The similarities of decay constants show that the Schottky barrier heights for both spin-up and spin-down electrons are the same, which is reasonable since the GaAs slab is essentially non-magnetic. This finding, however, is in contrast with results of calculations of the electronic properties of Co/Al₂O₃/Co magnetic tunnel junctions,³⁴ where different decay constants for the spin-polarized states at the Fermi energy in Al₂O₃, and therefore different potential barrier heights, were obtained for electrons of opposite spins. In terms of structure dependence, we find that the interfaces with intermixing of metal and semiconductor atoms tend to have longer decay lengths than abrupt interfaces, which is consistent with trends in the calculated Schottky barrier heights.

While detailed transport calculations, using, for example, the Landauer or Kubo formalisms, are needed for quantitative predictions regarding spin-polarized current, symmetry considerations allow us to make some qualitative arguments about the spin-injection process through the interface. Electrons tunnel from bulk states near the Fermi level in Fe through evanescently decaying gap states in the Schottky barrier region into states near the conduction band minimum in bulk GaAs (Fig. 9). The states participating in this transport process must be compatible by symmetry. In the approximation that transport across the interface is dominated by carriers

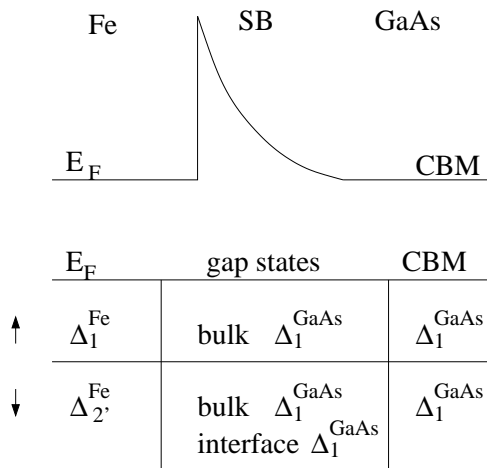


FIG. 9: Schematic flat-band diagram showing that electrons from bulk states near the Fermi level in Fe tunnel through decaying gap states in the Schottky barrier into states near the conduction band minimum in GaAs. (Note that the width of the barrier region is typically much larger than the decay length of the gap states.) In both majority and minority spin channels, there are bulk-like states in each region that are compatible by symmetry. Only in the minority spin channel are there interface-derived gap states of the right symmetry near the Fermi level.

with wave vector perpendicular to the interface, we focus on states with $\mathbf{k}_{\parallel} \approx 0$ (i.e., along the Δ direction in the cubic Brillouin zone of both GaAs and Fe). The 1×1 interface considered here has C_{2v} symmetry, and so does the lowest conduction band of GaAs (indexed as Δ_1^{GaAs}). In the Schottky barrier region, the most important bulk states in the complex band structure are those with the longest decay length. In GaAs, these states have Δ_1^{GaAs} symmetry as well.³⁵ Therefore, if we consider only bulk-like states, carriers must originate from states in the bulk Fe bandstructure that are compatible by symmetry with Δ_1^{GaAs} states. In the majority-spin band structure of Fe, the $d_{3z^2-r^2}$ -derived band, indexed as Δ_1^{Fe} , crosses the Fermi level and satisfies the symmetry requirement. In the minority-spin band structure, the d_{xy} -derived band, indexed as Δ_2^{Fe} , crosses the Fermi level and satisfies the symmetry requirement. Since the Δ_1^{Fe} band has some s character as well as $d_{3z^2-r^2}$ character, it is expected that the coupling of states across the interface will be stronger in the majority channel. Thus, considering only bulk-like states, the majority spin current would be expected to dominate. In fact, transport calculations based on the Landauer formalism support this conclusion.³⁶

However, in addition to bulk-like states, interface states may play a role in the tunneling process. The interface states in the vicinity of the Fermi level all have minority spin. Arising from $d_{3z^2-r^2}$ and d_{xy} orbitals on interface Fe sites, and resonant with the bulk Fe Δ_2^{Fe} minority band that crosses E_F , these states provide additional symmetry-compatible gap states for tunneling of minority spins through the barrier. Hence the presence

of these interface states close to the Fermi level could reduce the spin polarization of the tunneling current, or even reverse its sign. In Table V, we list the energy of the symmetry-compatible interface states within 0.5 eV of the Fermi level at the Γ point for different structural models. These states typically have dispersions of a few tenths of eV across the Brillouin zone. Since the proximity of these interface states to the Fermi level depends on the atomic structure at the interface, we expect the spin polarization of the injected current to be sensitive to interface structure as well. Measurements of the sign of the circular polarization of electroluminescence from Fe/GaAs spin LEDs indicate injection of minority spins,⁴ opposite to what is predicted from transport calculations for ideal junctions.³⁶ The present results indicate that details of the interface structure, such as the degree of intermixing and relaxation, likely contribute to this discrepancy.

TABLE V: Energy of symmetry-compatible minority-spin interface states within 0.5 eV of the Fermi level. Energies are in eV and measured relative to the Fermi level.

	As-terminated			Ga-terminated	
	Ideal	Relaxed		Ideal	Relaxed
Model A	0.15, 0.16, 0.37	0.31, 0.39, 0.39	N/A	0.43	
Model B	0.34, 0.41		0.16, 0.48	-0.02	0.12, 0.28

IV. CONCLUSIONS

We have investigated the electronic and magnetic properties of Fe/GaAs (001) interfaces using density functional calculations. Two structural models were compared: one with an abrupt interface and one with intermixing of metal and semiconductor atoms. Both As- and Ga-terminations were considered, and interlayer separations were relaxed. Due to differences in Fe-As and Fe-Ga bonding, the As-terminated structure favors the abrupt interface while the Ga-terminated structure favors intermixing at the interface. Magnetization profiles show bulk-like magnetic moments at the interfaces. In all cases, charge is transferred from Fe to GaAs, creating Schottky barriers that vary in height depending on details of the interface structure. In general, the SBHs are less sensitive to interlayer relaxations than to the nature of the interface, with intermixing of atoms at the interface leading to smaller n -type barrier heights. In all the structural models considered, the minority-spin Fe interface state induces states of Δ_1^{GaAs} symmetry within the semiconductor gap. These states lead to a reversal of the sign of the spin polarization of the density of states near the interface (compared to the Fe bulk), and this spin polarization of the density of states at the Fermi level persists well into the semiconductor. These interface-induced gap states (which also are likely to play a major

part in pinning of the Fermi level) provide an additional channel for tunneling of minority spins. The proximity of these interface states to the Fermi level, which affects the magnitude and possibly the sign of the spin polarization of the tunneling current, varies significantly with interface structure.

Acknowledgments

We would like to acknowledge support from the National Science Foundation, Grant No. DMR-0210717,

and the Office of Naval Research, Grant No. N00014-02-1-1046. We also thank the National Partnership for Advanced Computational Infrastructure for a supercomputing allocation.

-
- ¹ S. Datta and B. Das, Appl. Phys. Lett. **56**, 665 (1990).
² S. A. Wolf, D. D. Awschalom, R. A. Buhrman, J. M. Daughton, S. von Molnár, M. L. Roukes, A. Y. Chtchelkanova, and D. M. Treger, Science **294** 1488 (2001).
³ H. J. Zhu, M. Ramsteiner, H. Kostial, M. Wassermeier, H.-P. Schönherr, and K. H. Ploog, Phys. Rev. Lett. **87**, 016601 (2001).
⁴ A. T. Hanbicki, B. T. Jonker, P. M. G. Itskos, G. Kioseoglou, and A. Petro, Appl. Phys. Lett. **80**, 1240 (2002).
⁵ E. I. Rashba, Phys. Rev. B **62**, R16267 (2000).
⁶ C. H. Li, G. Kioseoglou, O. M. J. van 't Erve, A. T. Hanbicki, B. T. Jonker, R. Mallory, M. Yasar, and A. Petro, Appl. Phys. Lett. **85**, 1544 (2004).
⁷ C. Adelman, X. Lou, J. Strand, C. J. Palmström, and P. A. Crowell, Phys. Rev. B **71**, 121301(R) (2005).
⁸ X. Jiang, R. Wang, R. M. Shelby, R. M. Macfarlane, S. R. Bank, J. S. Harris, and S. S. P. Parkin, Phys. Rev. Lett. **94**, 056601 (2005).
⁹ W. H. Butler, X.-G. Zhang, Xindong Wang, Jan van Ek, and J. M. MacLaren, J. Appl. Phys. **81**, 5518 (1997).
¹⁰ M. Freyss, N. Papanikolaou, V. Bellini, R. Zeller, and P. H. Dederichs, Phys. Rev. B **66**, 014445 (2002).
¹¹ P. Vlaic, N. Baadji, M. Alouani, H. Dreyseé, O. Eriksson, O. Bengone, I. Turek, Surface Science **566**, 303 (2004).
¹² S. C. Erwin, S.-H. Lee, and M. Scheffler, Phys. Rev. B **65**, 205422 (2002).
¹³ S. Mirbt, S. Sanyal, C. Isheden, and B. Johansson, Phys. Rev. B **67**, 155421 (2003).
¹⁴ S. S. Kim, S. C. Hong, J. I. Lee, Phys. Stat. Sol. (a) **189**, 643 (2002).
¹⁵ G. Kresse and J. Furthmüller, Comput. Mater. Sci. **6**, 15 (1996); Phys. Rev. B **54**, 11169 (1996).
¹⁶ Y. Wang and J. P. Perdew, Phys. Rev. B **44**, 13298 (1991).
¹⁷ J. P. Perdew, K. Burke, and M. Ernzerhof, Phys. Rev. Lett. **77**, 3865 (1996).
¹⁸ D. Vanderbilt, Phys. Rev. B **41**, R7892 (1990).
¹⁹ H. J. Monkhorst and J. D. Pack, Phys. Rev. B **13**, 5188 (1976).
²⁰ D. K. Biegelsen, R. D. Bringans, J. E. Northrup, and L. E. Swartz, Phys. Rev. B **41**, 5701 (1990); N. Moll, A. Kley, E. Pehlke, and M. Scheffler, *ibid.* **54**, 8844 (1996); S. H. Lee, W. Moritz, and M. Scheffler, Phys. Rev. Lett. **85**, 3890 (2000).
²¹ J. Bardeen, Phys. Rev. **71**, 717 (1947).
²² M. Peressi, N. Binggeli, and A. Baldereschi, J. Phys. D **31**, 1273 (1998).
²³ D. E. Aspnes, Phys. Rev. B **14**, 5331 (1976).
²⁴ J. R. Waldrop, Appl. Phys. Lett. **44**, 1002 (1984).
²⁵ B. T. Jonker, O. J. Glembocki, R. T. Holm, and R. J. Wagner, Phys. Rev. Lett. **79**, 4886 (1997).
²⁶ C. S. Gworek, P. Phatak, B. T. Jonker, E. R. Weber, and N. Newman, Phys. Rev. B **64**, 045322 (2001).
²⁷ M. van Schilfgaarde and N. Newman, Phys. Rev. Lett. **65**, 2728 (1990).
²⁸ The Wigner-Seitz radii were chosen to be 1.355 Å for As, 1.402 Å for Ga, and 1.302 Å for Fe atoms.
²⁹ J. S. Claydon, Y. B. Xu, M. Tselepi, J. A. C. Bland, G. van der Laan, Phys. Rev. Lett. **93**, 037206 (2004).
³⁰ J. A. Stroschio, D. T. Pierce, A. Davies, R. J. Celotta, and M. Weinert, Phys. Rev. Lett. **75** 2960 (1995).
³¹ A. Biedermann, O. Genser, W. Hebenstreit, M. Schmid, J. Redinger, R. Podloucky, P. Varga, Phys. Rev. Lett. **76** 4179 (1996).
³² S. G. Louie and M. L. Cohen, Phys. Rev. Lett. **35**, 866 (1975).
³³ J. Tersoff, Phys. Rev. Lett. **52**, 465 (1984).
³⁴ I. I. Oleinik, E. Yu. Tsymbal, and D. G. Pettifor, Phys. Rev. B **62**, 3952 (2000).
³⁵ Ph. Mavropoulos, N. Papanikolaou, and P. H. Dederichs, Phys. Rev. Lett. **85**, 1088 (2000).
³⁶ O. Wunnicke, Ph. Mavropoulos, R. Zeller, P. H. Dederichs, and D. Grundler, Phys. Rev. B **65**, 241306(R) (2002).